Dynamical localization-delocalization transition of the reaction-diffusion front at a semipermeable cellulose membrane

Sung Hyun Park,[1] Hailin Peng,[1] Raoul Kopelman,[1] and Haim Taitelbaum[2]
[1]*Department of Chemistry, University of Michigan, Ann Arbor, Michigan 48109, USA*
[2]*Department of Physics, Bar-Ilan University, Ramat-Gan 52900, Israel*
(Received 13 August 2006; published 26 February 2007)

We study the kinetics of the reaction front in the $A+B\rightarrow C$ reaction-diffusion system with reactants initially separated by a semipermeable membrane. The semipermeable membrane allows only one reactant species to go through ("penetrating species") while the other reactant species is sterically prohibited from penetration. Theoretically, the ratio of the diffusive fluxes of the two species has been defined before as a control parameter and it was predicted [Chopard *et al.*, Phys. Rev. E **56**, 5343 (1997)] to give rise to a localization-delocalization transition of the reaction front. In this paper we show the experimental realization of a dynamical localization-delocalization transition, in a system consisting of the reactants Ca^{2+} and calcium green-1 dextran, separated by a finite-sized cellulose membrane. The dynamical transition results from the continuous change in time of the flux of the penetrating species at the reaction boundary. Here this time-dependent flux is attributed to the free diffusion of the penetrating species through a membrane with a finite thickness. The dynamical transition is exemplified by the kinetic behavior of the front characteristics which exhibits several time regimes — an early time, an intermediate time, and an asymptotic time regime. The crossover times between these regimes are found to depend on the membrane thickness, a parameter not considered before to our knowledge. Monte Carlo simulations show good agreement with the finite-time experiments.

DOI: 10.1103/PhysRevE.75.026107 PACS number(s): 82.20.Wt, 82.20.Db, 66.30.Ny

I. INTRODUCTION

The presence of a reaction front is a characteristic feature of a variety of physical, chemical, and biological processes. For example, the process $A+B\rightarrow C$ exhibits a front (i.e., a spatially localized region where the production of C is nonzero) provided the diffusing reactants A and B are initially separated in space. Interest in these fronts has increased recently since it has been realized that pattern formation in the wake of a moving front is a fairly general phenomenon. A classical case associated with the $A+B\rightarrow C$ front reaction is the Liesegang-band formation [1] which is thought to be a complex process of interplay between the dynamics of the reaction front and the nucleation kinetics of the precipitate (C). The first stage in understanding pattern formation in such processes is the description and calculation of the properties of the reaction zone, i.e., answering the question of where and at what rate the reaction product C appears. Gálfi and Rácz [2] were the first to suggest scaling laws for the long-time behavior of the product C (i.e., the front). Their seminal work was followed, theoretically as well as experimentally, by many authors [3–15].

Gálfi and Rácz [2] formulated the problem in terms of the following set of mean-field reaction-diffusion equations for the local concentrations $a(x,t)$ and $b(x,t)$:

$$\dot{a} = D_a \nabla^2 a - kab,$$

$$\dot{b} = D_b \nabla^2 b - kab, \tag{1}$$

where D_a and D_b are the diffusion coefficients of the reactants, and k is the microscopic reaction rate constant. The system is subject to an initial separation of reactants in space, which is expressed mathematically as

$$a(x,0) = a_0[1 - H(x)],$$

$$b(x,0) = b_0 H(x), \tag{2}$$

where a_0 and b_0 are the initial reactant concentrations and $H(x)$ is the Heaviside step function. Equation (2) implies that, at time $t=0$, the species A molecules are homogeneously distributed on the left-hand side ($x<0$), and the B on the right ($x>0$).

Gálfi and Rácz [2] assumed that the local production rate $R(x,t)$ of C takes a scaling form inside the reaction zone at the long-time limit:

$$R(x,t) = R(x_f,t) F\left(\frac{x - x_f(t)}{w(t)}\right),$$

$$w(t) \sim t^{\alpha}, \quad R(x_f,t) \sim t^{-\beta}, \tag{3}$$

where $R(x_f,t)$, the front height, is the value of $R(x,t)$ at the front center location $x_f(t)$, the latter scales with time as $t^{1/2}$, due to the diffusion. The scaling function F is then a function of the distance from the front center relative to the front width $w(t)$. The production rate $R(x,t)$ within the reaction zone depends on the incoming diffusive fluxes of A and B, as well as on the decrease of these very fluxes due to the $A+B$ reaction. These two opposite trends give rise to new exponents for the width ($\alpha=1/6$) and the height ($\beta=2/3$) of the reaction zone [2]. The global reaction rate $R(t)=\int_{-\infty}^{+\infty} R(x,t)dx$ scales like $t^{-1/2}$. These predictions, which were argued to be valid for dimensions $d_c \geq 2$ [3], have been verified both numerically [4,5] and experimentally [5–7]. It was also shown [4,8,9] that when one of the species is static the width is asymptotically a constant, and the height decreases as $t^{-1/2}$. The early-time behavior and its nontrivial

TABLE I. The theoretical asymptotic time scaling exponents of $x_f(t)$, $w(t)$, and $R(x_f,t)$ for a zero-thickness semipermeable wall separating the reactants at $t=0$, as predicted in [15].

	$x_f(t)$	$w(t)$	$R(x_f,t)$
$r<0$	0	0	−1/2
$r=0$	1/6	1/6	−2/3
$r>0$	1/2	1/6	−2/3

consequences have been studied extensively, using perturbation theory, computer simulations and experiments [10–14].

Chopard *et al.* [15] studied a zero-thickness *semipermeable* wall as the boundary at $x=0$, where the A particles can penetrate the wall, but the B's cannot. They showed that the control parameter for the asymptotic behavior of the reaction front in the presence of a semipermeable membrane is the ratio of the diffusive fluxes, r, defined as

$$r = 1 - \frac{b_0\sqrt{D_b}}{a_0\sqrt{D_a}}. \tag{4}$$

Their theory predicts three different asymptotic behaviors of a reaction front for the following three cases. (1) $r>0$, *i.e., the flux of A is greater than that of B.* The resistance of the membrane can be ignored, so this case is the same as without a membrane. The reaction front moves to the right, B side, characterized by the same exponents as above ("delocalized front"). (2) $r<0$, *i.e., the flux of B is greater than that of A.* If no membrane exists, B should be the invading species, and the reaction front will move toward the A side. However, with the semipermeable membrane, the abundant B's react immediately with A's that successfully penetrate through the membrane, and the reaction front will remain at the membrane ("localized front"), with its width predicted not to expand in time. (3) $r=0$, *i.e., the flux of B is equal to that of A.* The reaction front is predicted to move slightly toward the B side at a rate of $t^{1/6}$, and the width of the reaction front slowly expands, scaling also as $t^{1/6}$. The value of $r=0$ was therefore considered as a critical point where a dynamical transition between a delocalized and a localized front occurs. To clarify the different parameter regimes, a summary of the theoretical scaling exponents of $x_f(t)$, $w(t)$, and $R(x_f,t)$, *below*, *at*, and *above* the critical point, can be found in Table I.

In this paper we study experimentally and numerically the reaction-diffusion front characteristics in the presence of a finite-size semipermeable membrane. We do so by using a complex formation reaction at a cellulose membrane, with a penetration cutoff at a given molecular weight of the chelating agent, so that small enough particles can diffuse through, while larger molecules cannot. This resembles the situation in many reactions in biological cells, which involve an ion and a large molecule, such as a protein or DNA. Often the large molecule cannot move freely but the ion can [16].

In earlier experimental investigations of the reaction-diffusion front with initially separated reactants, the boundary at $x=0$ was either just due to the direct contact of the A and B reactants which were injected from both sides of a long capillary [5,6], or was a physical boundary such as an optical fiber of negligible thickness inserted in gel-free experiments done in a Hele-Shaw cell geometry [7]. However, the experimental use of a semipermeable membrane, as done in our case, introduces another complexity into the system, because this membrane has a finite thickness (of order of 30 μm). As we shall see below, this gives rise to a *dynamical* localization-delocalization transition, resulting from the fact that the invading species must first diffuse through the membrane itself, prior to its first encounter with the other species. This introduces several new kinetic regimes into the problem, which will be discussed in detail below. It is worth pointing out that the current dynamical transition caused by the presence of a semipermeable membrane is different from the transition between a classical early-time regime and a nonclassical asymptotic regime [10,11].

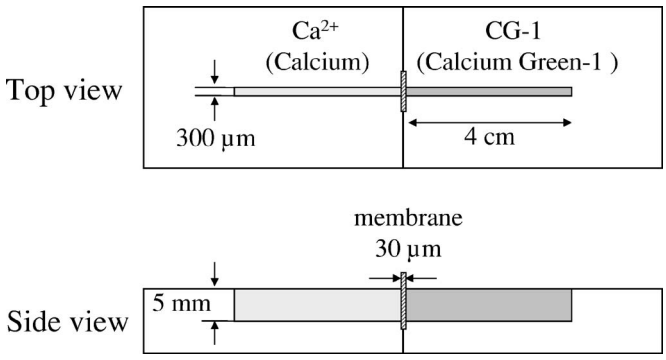

FIG. 1. A schematic of the reactor with a membrane.

The paper is organized as follows. In Sec. II we describe the experimental system and the experimental results. In Sec. III we present our Monte Carlo simulations and Sec. IV is devoted to the membrane thickness effect. Section V is a summary.

II. EXPERIMENTS

The chemical reaction monitored is between $Ca^{2+}(A)$ and calcium green-1 dextran 10 000 (CG-1) (B). A cellulose membrane, with a cutoff molecular weight at 1000 Da, is placed between the two reactants. The small Ca^{2+} ions can diffuse freely through the membrane into the CG-1 side, while the large CG-1 molecules are prohibited from penetrating through the membrane. The reactant concentrations in the bulk solutions are $[Ca^{2+}]=1.0\times10^{-4}$ M, and $[\text{CG-1}]=1.0\times10^{-5}$ M. To avoid any charge effect, 0.1 M KCl is added to both solutions. In order to avoid possible convection, we prepare the reactants in a mixture of glycerol and water. We use a 60% (wt/wt) glycerol concentration, which is about ten times more viscous than pure water [17].

The home-made optically transparent acrylic reactor consists of two separate half pieces, each of which has a straight, thin, rectangular channel for reactant solution. The channel size is about 300 μm (width) × 5 mm (depth) × 4 cm (length) on each half piece (see Fig. 1). We inject a sample solution into the channel on each separate half piece using a

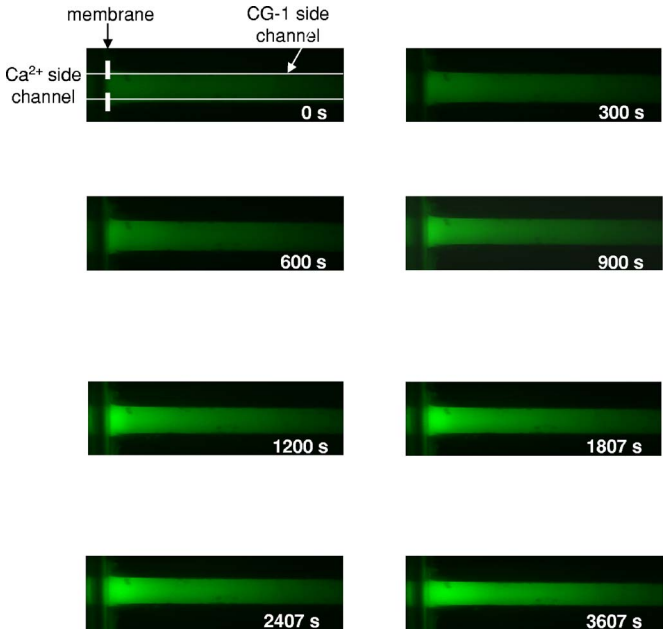

FIG. 2. (Color online) CCD snapshots at $t=0$, 300, 600, 900, 1200, 1807, 2407, and 3607 s.

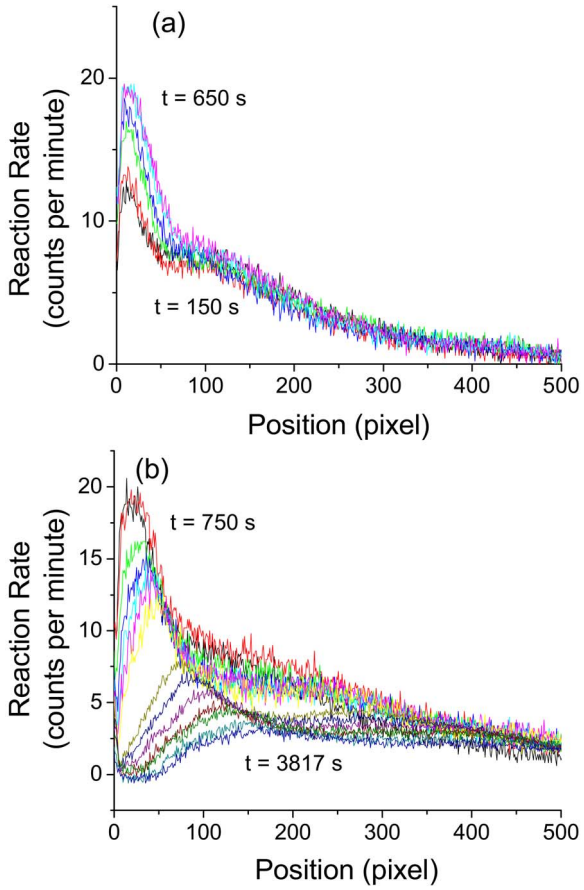

FIG. 3. (Color online) The spatial profiles of the reaction front from the experiments. (a) Early time regime (profiles are shown at $t=150$, 250, 350, 450, 550, and 650 s). The front is localized and its height increases. (b) Later, transient time regime (shown at $t=750$, 850, 950, 1050, 1150, 1250, 1350, 2017, 2317, 2617, 2917, 3217, 3517, and 3817 s). The front begins to delocalize and detaches from the wall. The height is drastically decreasing, manifesting the depletion zone effect, and the front width is growing significantly.

syringe. After the sample injection, the top part of each channel is sealed with transparent tape to prevent evaporation. Next, a small piece ($\sim 4\times 6$ mm^2) of cellulose membrane with a thickness of ~ 30 μm, washed in ethylene diamine tetra-acetic acid (EDTA) and water, to remove impurity ions, is put on one side of a channel (usually the dye side) on a half piece, then the other half piece (the calcium side) is brought into contact with the other side of the membrane. Upon crossing the membrane, the calcium ion binds with the chelating dye CG-1 and dramatically increases the fluorescence intensity of the now modified dye [18]. The reaction product is monitored using a microscope equipped with a charge-coupled device (CCD) camera. Some typical snapshots are shown in Fig. 2. Each snapshot reflects an accumulation of the products produced from $t=0$ up to that time. Thus the higher fluorescence intensity regions reflect the total amount of products produced up to that time. To obtain front profiles from these snapshots, we consistently subtract two snapshots (an earlier from a later one) to obtain the net amount of products formed during the time interval between the two snapshots, and then divide by that time interval, so as to convert it to the local reaction rate or profiles of the reaction front.

Figure 3 shows typical experimental profiles of the reaction front. Since the calcium ion, a penetrating species, has a higher initial bulk concentration, as well as a larger diffusion coefficient, compared to the CG-1 dye, i.e., we are in the limit of $r>0$ [Eq. (4)], and thus the front is expected to behave asymptotically in the same way as when there is no membrane. However, as shown in Fig. 3(a), the position of the reaction front seems almost static during the earlier period of time. The height of the reaction front increases in time during the same period. At later times, as shown in Fig. 3(b), the reaction front height begins to decrease and the front finally starts to move away from the membrane. This is what is meant by the term *dynamical* localization-delocalization transition. This transition results from the fact that, in this system, the control parameter r is in fact *time dependent*, which is a direct consequence of the finite thickness of the membrane. Note that, in these figures, the actual reaction front is the main peak on the left. The right part, a shoulder peak, is possibly related to the fluorescence background of the unreacted dye, and is not considered to be part of the front.

Figure 4 is a schematic description of the situation. The calcium concentration (hence the flux) entering the dye side should increase gradually in time. Initially the calcium flux is lower than that of the dye ($r<0$), although the initial condition in the entire system (bulk) is still $r>0$ (cases 1 through 3 in Fig. 4). In this case, the front position is expected to be static, just next to the wall (see Table I). The front height keeps increasing as more particles are passing through the membrane boundary (at $x=0$ in Fig. 4). This is regarded as an early-time regime, where the presence of the barrier interferes with the normal development of a depletion zone, thus it must correspond to a behavior that is different from the

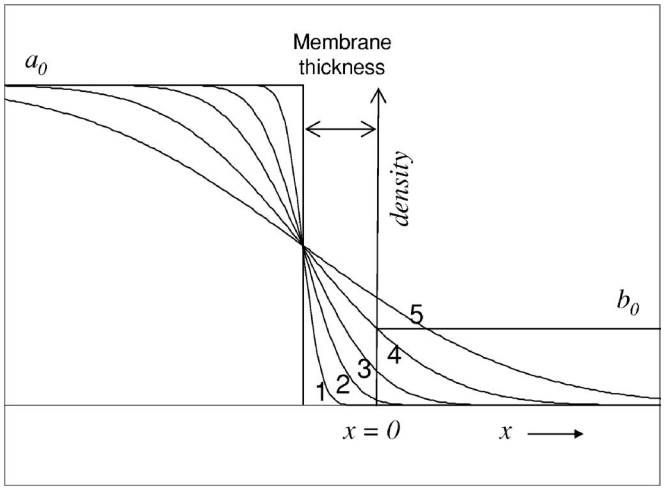

FIG. 4. A schematic of the penetration of A species through an empty semipermeable membrane into the B side. The concentration, hence the flux, of the A species increases gradually with time (cases 1 to 5) at the initial boundary $x=0$ of the reaction front. For simplicity of this sketch, the B profile is kept constant in time.

asymptotic decrease of the height shown in Table I.

The increasing, in time, calcium flux means that, at some point, the system will reach, at least momentarily, a "critical point" where the fluxes of the two reactants are equal, i.e., effectively, $r=0$ (case 4 in Fig. 4). Immediately thereafter, as the calcium flux continues to increase in time, the system will reach the case of $r>0$ (case 5 in Fig. 4), and the delocalized front is finally expected to behave in accordance with what is expected for the bulk initial condition (see Table I).

In our experimental setup, the typical time for Ca^{2+} ions to cross the membrane is found to be ~15 min, that is, after the two half reactors are brought into contact, the first signal of the reaction front is detected after ~15 min. This is $t=0$ of our experiment. However, even when the very early calcium flux finally reaches the other side after these ~15 min (just after case 1 in Fig. 4), the effective value of r is still changing, as explained above. The moment when the flux of the penetrating species (calcium) becomes just higher than that of the blocked species (dye) (just after case 4 in Fig. 4) would experimentally be the time when the static front starts to move "at a significant speed," i.e., as $t^{1/2}$ $(r>0)$, namely, when the dynamical localization-delocalization transition has already occurred.

Figure 5 shows the overall data from the experiments for the position, the height, and the width of the front, denoted by $x_f(t)$, $R(x_f,t)$, and $w(t)$, respectively. These plots clearly indicate several time regions. In Fig. 5(a) we show the results for the reaction front center. In the first ~700 s the front is stationary, i.e., localized. Then it detaches from the wall and moves at a significantly large pace. This is interpreted as the dynamical transition between the short-time $r<0$ region (up to ~700 s), and the asymptotic time region $(r>0)$ when x_f should grow in time as $t^{1/2}$. Due to the instability of the experimental system at very long times, we could not obtain reliable experimental data for such long time scales, so we support the data interpretation in this time regime by numerical simulations (below). We should mention again that all the

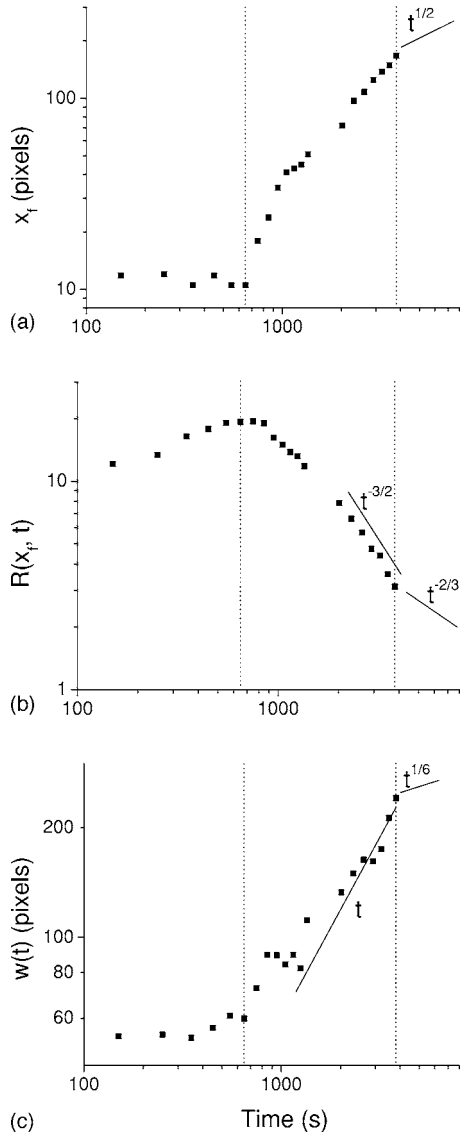

FIG. 5. The overall time scalings from the experiments for three characteristics of the front: (a) location $x_f(t)$, (b) height $R(x_f,t)$, and (c) width $w(t)$.

time points are measured from the first reaction encounter between the A and B particles.

Similar behavior of multiple time regimes for the reaction front center is seen in Figs. 5(b) and 5(c) for the height $R(x_f,t)$ and the width $w(t)$ of the reaction front, respectively. To determine the width of the experimental reaction front in the presence of the shoulder peak located to its right (see Fig. 3), we follow the signal decrease with increasing position coordinate in Fig. 3. Once the signal starts to increase again, we cut the data parallel to the y axis. We take the left side as the front and measure the width of the left side. At the earlier times, the height increases and the width remains stationary, as more and more particles are crossing the membrane; but the front still remains localized next to the wall. After about 800 s, the front becomes dynamically delocalized, its height decreases as $t^{-3/2}$, and its width increases *linearly* in time. Again, we interpret this region as a transient region, prior to the final asymptotic time region, where we expect the height

and the width to behave as $t^{-2/3}$ and $t^{1/6}$, respectively. This interpretation is also confirmed by the numerical simulations (below). It is interesting to note, however, that both sets of exponents for the height (β) and the width (α) [Eq. (3)] satisfy the universal scaling relation first introduced by Gálfi and Rácz [2],

$$\alpha - \beta = -1/2, \tag{5}$$

where the $-1/2$ exponent on the right-hand side is the exponent of the asymptotic behavior of the *global* rate $R(t)$. This means that in both the transient and the asymptotic regions, the global rate decreases as $t^{-1/2}$, whereas the exponents of the height and the width differ, but still obey the relation (5).

III. MONTE CARLO SIMULATIONS

We performed Monte–Carlo simulations on a rectangular lattice of size 40×1000, which is sufficiently long in the x direction in order to mimic an infinite system. The membrane, having a thickness (actually width) of 10 lattice units, is located in the middle of the lattice, perpendicular to the x direction. Once the two kinds of reactants collide, the reaction happens, creating a product C, and the A and B particles are removed from the lattice. We record the time and location where the product C is created. The latter is assumed neither to block the A or B diffusion (due to its relatively small C concentration), nor to further diffuse in the system. The initial concentration of A (permeable species) is 0.5 and the concentration of B (impermeable species) is 0.125. We choose the A concentration to be four times that of B to make sure that, eventually, on the B side, the A concentration will be higher than the concentration of B. Initially, there is no particle within the membrane. The mobilities (i.e., diffusivities) of the reactants are taken to be either equal or different, using an algorithm where at each time step a particle can remain in its site with a certain probability. We also considered a version in which the B particles were static, as discussed below. The results are averages from 5000 runs.

Figure 6 shows the reaction front profiles at different times for the case of equal diffusivities. Just as we saw from our experiments, one can see several time regimes. At the earliest times, the height of the reaction front increases with time and the peak stays static just next to the membrane [Fig. 6(a)]; then the height starts to decrease but the peak is still localized next to the wall [Fig. 6(b)]. Finally, the front detaches from the wall and starts to move away [Fig. 6(c)]. The corresponding characterizations of the reaction front are shown in Fig. 7. The front location in Fig. 7(a) reflects the static nature of the front at early times, before approaching the limit of the $t^{1/2}$ scaling asymptotically. The height of the front in Fig. 7(b), after increasing at the beginning, as mentioned above, seems to decrease strongly, as $t^{-3/2}$, in an intermediate time range, and finally decreases according to the theoretical prediction for the asymptotic time limit, as $t^{-2/3}$. The front width in Fig. 7(c) appears to be static at early times, and then undergoes a very fast transition, growing in time linearly, to an asymptotic $t^{1/6}$ time scaling. Figure 7(d) for the global reaction rate $R(t)$ shows that, in both the transient region (which is still part of the localized phase), as well as in the asymptotic time limit (which represents the delocalized phase), the global rate $R(t)$ decreases as $t^{-1/2}$. This confirms that the exponents of the height and the width of the front satisfy the relation (5) in both regions.

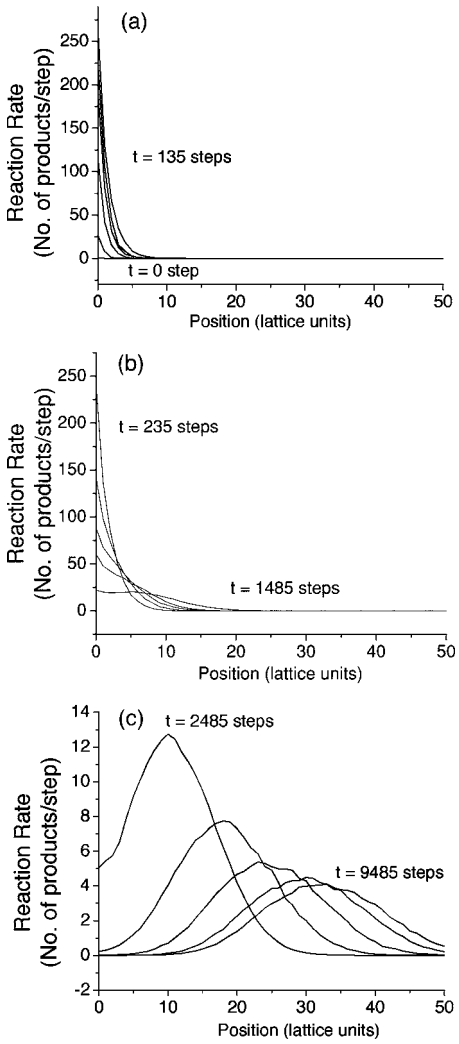

FIG. 6. Monte Carlo results of the reaction front profiles. Three time regimes are observed: (a) at the very beginning, the peak height increases and the peak position remains at the membrane wall (profiles are shown at $t=0$, 20, 40, 60, 80, and 135 steps); (b) next, the peak height decreases but the peak is still localized at the membrane wall (shown at $t=235$, 435, 635, 835, and 1485 steps); (c) finally, the peak position moves away from the membrane (shown at $t=2485$, 4485, 6485, 8485, and 9485 steps).

We repeated these studies for different diffusivities of A and B and all results confirm the dynamical localization-delocalization transition, manifested mainly by the existence of the intermediate time regime. It represents a transition, a crossover behavior, between the early-time, localized front, and the asymptotic, delocalized front. In fact, it combines properties of both regions. While the front is still localized (as in the early time regime), its width increases and its height decreases (as in the asymptotic time limit). Since the front is still localized at the membrane boundary, the A's are feeding it at a constant rate, and hence the width grows linearly, with $\alpha \approx 1$. This "too wide" zone implies a rapid decay

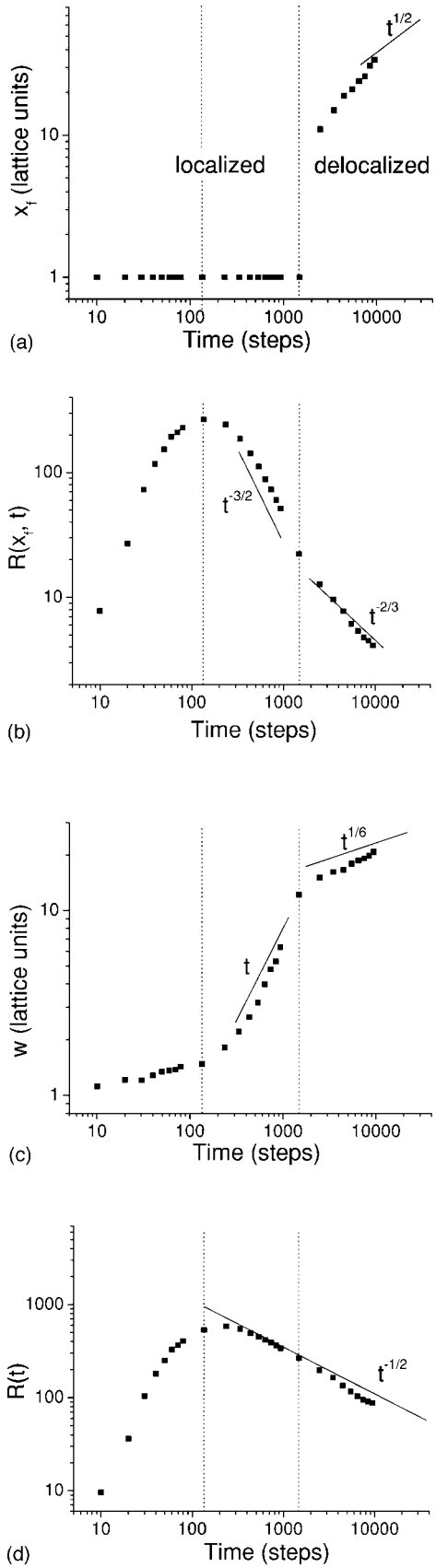

FIG. 7. The overall time scalings from Fig. 6 for four characteristics of the front: (a) location $x_f(t)$, (b) height $R(x_f,t)$, (c) width $w(t)$, and (d) global rate $R(t)$.

of its height, exemplified by the $\beta \approx 3/2$ exponent, in order to keep the relation (5). At later times, when the front detaches from the wall, the feeding of the A's is not immediate; hence we get the Gálfi-Rácz exponents.

Similar results were obtained in simulations for finite-size membranes where the B particles are static. The only difference was found to be in the asymptotic limit. In the originally formulated initially-separated reactants system [2], the height and width exponents are known [4,8,9] to be different from the case where both reactants are mobile. The width is asymptotically a constant, and the height decreases as $t^{-1/2}$. This different behavior has been obtained by us for the finite-size semipermeable wall in the last kinetic regime, i.e., the asymptotic limit. The above study was motivated by the fact that, in the experimental system described above, the B particles are much less mobile with respect to the A particles. Thus, the limit of B being static could be considered to be relevant. However, as mentioned above, we were not able to obtain experimental data in the asymptotic limit, which is the only time regime where these two systems differ.

In general, the agreement between all sets of simulations with the experimental data is encouraging, as all show the multiple time regime behavior. A slight deviation appears in the results for the position of the front $x_f(t)$, which seems to start detaching from the wall already at the intermediate time regime.

IV. EFFECTS OF THE MEMBRANE THICKNESS

In order to study the effect of the membrane thickness, Monte Carlo simulations have been carried out for various membrane thicknesses (W). Other parameters (lattice size, initial reactant concentrations, diffusivities, boundary conditions, number of runs, etc.) of all the simulations have been kept the same as before. The time range monitored was from 1 to 10 000 time steps.

If the membrane width is zero, the reaction will start right away at the membrane. In all other cases it will take some time before the A particles penetrate through the membrane, a time interval which should depend on the membrane thickness, according to Einstein's law, as W^2. Let us denote this time by τ_0, which is in fact the time origin ($t=0$) for all the data presented above. We can then define three characteristic times in the problem. The first is τ_0, which is the time when the first encounter between A and B occurs. This is the start of the reaction-diffusion process ($t=0$). Then we have τ_1, which is the crossover time between the short-time limit and the transient limit. At this time point, which is within the localized phase, the height of the front starts to decrease, as enough reactions have already occurred and the depletion zone starts to become effective. Finally we define τ_2, which designates the phase transition to the delocalized phase and eventually to the asymptotic limit. Correspondingly, one can define these durations of each time regime, i.e., τ_0, which is the duration of the first crossing of the membrane (prior to the early time regime); $\tau_1 - \tau_0$, which is the duration of the early time reaction regime; and finally $\tau_2 - \tau_1$, the duration of the intermediate time regime.

In Fig. 8 we show, on a log-log scale, the dependence of these three crossover times [Fig. 8(a)], as well as the three

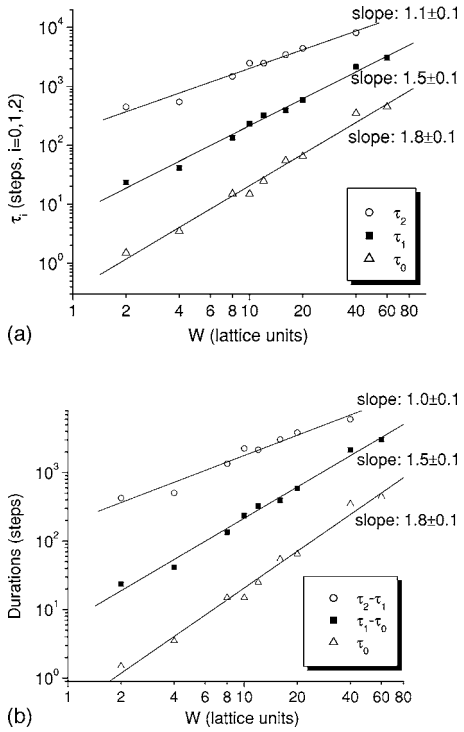

FIG. 8. The dependence of (a) the three crossover times and (b) the three durations, on the membrane thickness W, from Monte Carlo simulations with equal reactant diffusivities.

durations [Fig. 8(b)], on the membrane thickness, as obtained by our numerical simulations. While τ_0 seems to obey Einstein's law (close to exponent 2), the two other crossover times, as well as the two other durations, exhibit a weaker dependence on the membrane thickness, which reflects the nontrivial nature of the multiple kinetic time regimes of the problem. The plots of the durations $\tau_1-\tau_0$ and $\tau_2-\tau_1$ in Fig. 8(b) look very similar to those of τ_1 and τ_2, respectively, in Fig. 8(a), simply because the final time of each regime is much larger than the initial time, implying that these durations are practically determined by the crossover time at the end of each regime. It should also be noted that Fig. 8 was produced for the case of equal reactant diffusivities; however, the results were similiar for different diffusivities of the reactants.

V. SUMMARY

In this paper, we studied the behavior of the reaction front for an elementary bimolecular reaction $A+B\rightarrow C$ with a semipermeable membrane. In the experiments on calcium ions reacting with calcium green through a cellulose membrane we observe at least two time regimes for the dynamics of the reaction front. This is a reflection of the continuous change in time in the value of the *effective* control parameter r, from $r<0$, through $r=0$, to $r>0$. This change in the control parameter is attributed to the free diffusion of the penetrating species through a nonzero, finite thickness membrane, prior to the reaction with the other species. The results have been verified by Monte Carlo simulations, and the latter show in fact that there exist three distinct time regimes, ranging over the entire time domain: The first is a short-time, localized phase, when the reaction production is increasing; the second is a transient time regime, still within the localized phase of the system, where the depletion zone starts to affect the kinetics; and the third is the asymptotic time regime, when the delocalized phase of the kinetics takes place, and thus the reaction front moves away from the membrane. The last regime could not be monitored experimentally, but did show up in the simulations.

We analyzed and discussed the characteristics of the reaction front in all three time regimes, the first two exhibiting a localized front. In particular we showed the interesting behavior occurring in the transient time regime, where the front characteristics (height and width) seem to change at a rate much different from the asymptotic behavior, where the front is delocalized. We also looked at the various crossover times in the system as a function of an additional, new parameter, introduced for this class of systems, which is the thickness of the initial boundary between the reactants. This barrier width parameter is indispensable for any realistic description of experimental situations.

ACKNOWLEDGMENTS

Support from NSF DMR Grant No. 0455330 (R.K.) and ISF Grant No. 1342/04 (H.T.) is gratefully acknowledged.

[1] R. E. Liesegang, Naturwiss. Wochenschr. **11**, 353 (1896).
[2] L. Gálfi and Z. Rácz, Phys. Rev. A **38**, 3151 (1988).
[3] S. Cornell, M. Droz, and B. Chopard, Phys. Rev. A **44**, 4826 (1991).
[4] Z. Jiang and C. Ebner, Phys. Rev. A **42**, 7483 (1990).
[5] Y.-E. L. Koo, L. Li, and R. Kopelman, Mol. Cryst. Liq. Cryst. **183**, 187 (1990).
[6] Y.-E. L. Koo and R. Kopelman, J. Stat. Phys. **65**, 893 (1991).
[7] S. H. Park, S. Parus, R. Kopelman, and H. Taitelbaum, Phys. Rev. E **64**, 055102(R) (2001).
[8] Z. Koza, Physica A **240**, 622 (1997).
[9] M. Z. Bazant and H. A. Stone, Physica D **147**, 95 (2000).
[10] H. Taitelbaum, S. Havlin, J. E. Kiefer, B. Trus, and G. H. Weiss, J. Stat. Phys. **65**, 873 (1991).
[11] H. Taitelbaum, Y.-E. L. Koo, S. Havlin, R. Kopelman, and G. H. Weiss, Phys. Rev. A **46**, 2151 (1992).
[12] Z. Koza and H. Taitelbaum, Phys. Rev. E **54**, R1040 (1996).
[13] H. Taitelbaum and Z. Koza, Philos. Mag. B **77**, 1389 (1998).
[14] H. Taitelbaum and Z. Koza, Physica A **285**, 166 (2000).
[15] B. Chopard, M. Droz, J. Magnin, and Z. Rácz, Phys. Rev. E **56**, 5343 (1997).
[16] For example, see J. W. Kimball, *Biology*, 6th ed. (Wm. C. Brown Publishers, Dubuque, IA, 1994).
[17] *Handbook of Chemistry and Physics*, 82nd ed., edited by D. Lide (CRC Press, Boca Raton, FL, 2001).
[18] R. P. Haugland, *The Handbook: A Guide to Fluorescent Probes and Labeling Technologies*, 10th ed. (Molecular Probes Inc., Eugene, OR, 2005).